Bayona, V., Moscoso, M., & Kindelan, M. (2012). Gaussian RBF-FD weights and its corresponding local truncation errors. *Engineering Analysis with Boundary Elements*, 36(9), 1361-1369.

DOI: 10.1016/j.enganabound.2012.03.010

Gaussian RBF-FD weigths and its corresponding local truncation errors

Victor Bayona, Miguel Moscoso, Manuel Kindelan.

January 25, 2012

Abstract

In this work we derive analytical expressions for the weights of Gaussian RBF-FD and Gaussian RBF-HFD formulas for some differential operators. These weights are used to derive analytical expressions for the leading order approximations to the local truncation error in powers of the inter-node distance h and the shape parameter .

We show that for each differential operator, there is a range of values of the shape parameter for which RBF-FD formulas and RBF-HFD formulas are significantly more accurate than the corresponding standard FD formulas. In fact, very often there is an optimal value of the shape parameter $^{+}$ for which the local error is zero to leading order. This value can be easily computed from the analytical expressions for the leading order approximations to the local error. Contrary to what is generally believed, this value is, to leading order, independent of the internodal distance and only dependent on the value of the function and its derivatives at the node.

1 Introduction

Radial basis functions (RBFs) were first used as an efficient technique for interpolation of multidimensional scattered data (see [8] and references therein). Later, it became popular as a truly mesh-free method for the solution of partial differential equations (PDEs) on irregular domains. This application of RBFs was first proposed by Edward Kansa [13, 14] and it is based on collocation in a set of scattered nodes. The main advantages of the method are ease of programming and potential spectral accuracy, but its main drawback is ill-conditioning of the resulting linear system.

To overcome this drawback a local RBF method was independently proposed by several authors [17, 18, 20]. The method is based on approximating the solution as a linear combination of a set of identical RBFs translated to a set of (scattered) RBF centers. However, the approximation is local, so it is carried out within a small influence domain instead of a global one. Thus, the resulting linear system is sparse, overcoming the ill-conditioning of the global method, at the cost of losing its spectral accuracy.

The local RBF method can also be considered as a generalization of the classical FD method. In the FD method the weights are computed using polynomial interpolation, while in the local RBF method they are computed by fitting an RBF interpolant through a grid point and a small number of its nearest neighbors. Since both, FD and local RBF formulas are identical in form, we will refer to the local RBF method as the RBF finite difference (RBF-FD) method, as in [20].

In Hermite interpolation the objective is to find a polynomial that interpolates both the value of the function at some neighboring nodes and the value of some derivatives at the same or different nodes. Taking the derivative of these interpolation formulas one derives Hermite finite difference formulas (HFD). Analogously to what is done with RBF-FD, we can use RBF's instead of polynomials for interpolation. We will refer to the resulting method as the RBF Hermite finite difference (RBF-HFD) method [20].

Many of the RBFs used in practical applications contain a shape parameter that has to be chosen a priori. It is well known that the accuracy of the approximated solution strongly depends on its value. Thus, the problem of how to select appropriate values for the shape parameter has been of primary concern both from the theoretical and the application points of view. In a recent paper [1] we derived analytical approximations to the local approximation error for 1D and 2D differential operators (for structured and non-structured nodes) using multiquadrics as RBFs. These formulas were then used to propose efficient algorithms for the selection of either an optimal (constant) value of the shape parameter that minimizes the approximation error [2], or an optimal (node dependent) value of the shape parameter that minimizes the local approximation error [3]. In this paper we carry out a similar analysis to the one performed in [1] but using Gaussians instead of multiquadrics as RBFs. The formulas for the local approximation error that we derive below can then be used to compute the optimal value of the shape parameter (both constant and variable) in a way similar to that used in [2, 3].

There are not too much work relating to the RBF-FD method using Gaussians as RBFs. One should mention the work of Flyer and Wright [11] and Davydov and Oanh [9, 10] from the application point of view, and the work of Wright and Fornberg [20, 12] and Boyd and Wang [4] from the analytical point of view. With respect to the value of the optimal shape parameter one should mention the work of A.H.-D. Cheng [5] which used the error formulas derived by Madych [15] to find analytical expressions for the value of c which minimizes the error for a given internodal distance h. However, these formulas are for the global RBF method, not for the local RBF-FD method, and in that case, the optimal shape parameter is independent of the particular function f whose derivatives are being approximated.

The paper is organized as follows: in Section 2 it is described the RBF-FD and RBF-HFD formulation; in Section 3 it is shown the weights and the local truncation errors, first for the RBF-FD method (subsections 3.1.1, 3.1.2, 3.1.3) and then for the RBF-HFD method (subsections 3.2.1, 3.2.2). In Section 4 it is discussed the main conclusions of the work.

2 RBF-FD formulation

2.1 RBF-FD method

In this section we describe how the RBF-FD formulas are derived and how the weights can be exactly computed. Consider a differential operator $\mathcal{L}[\,]$ and a stencil consisting of n scattered nodes $\{\mathbf{x}_1, \mathbf{x}_2, \ldots, \mathbf{x}_n\}$. For a given node $\mathbf{x} = \mathbf{x}_j$ ($1 \leq j \leq n$), the differential operator can be approximated by the formula

$$\mathcal{L}[u(\mathbf{x}_j)] \approx \sum_{i=1}^{n} \lambda_i u(\mathbf{x}_i), \tag{1}$$

where λ_i are the weighting coefficients. In the standard FD formulation, these coefficients are computed using polynomial interpolation. In the RBF-FD formulation, RBF interpolants are used instead. Thus,

$$u(\mathbf{x}) = \sum_{i=1}^{n} \lambda_i \phi(\|\mathbf{x} - \mathbf{x}_i\|), \tag{2}$$

where $\|\cdot\|$ is the euclidean norm and $\phi(r)$ is some radial function. The unknown weighting coefficients λ_i can be determined by solving the system of linear equations,

$$\mathcal{L}[\phi(\|\mathbf{x}_k - \mathbf{x}_j\|)] = \sum_{i=1}^{n} \lambda_i \phi(\|\mathbf{x}_k - \mathbf{x}_i\|), \quad k = 1, \ldots, n, \tag{3}$$

which is obtained doing some algebra after substituting (2) in (1). It is well known [19] that the Gaussian function is a positive definite RBF and, therefore, the linear system resulting from interpolation is always invertible. For conditionally positive definite RBFs (like generalized multiquadrics) a polynomial term has to be added in order to guarantee invertibility of the resulting system (a constant for standard multiquadric). However, although it is not needed for invertibility, adding a constant term to the RBF interpolant (2) guarantees that a constant function is interpolated exactly. In this case, the unknown weighting coe cients $_i$ can be calculated by solving the system of linear equations

$$
\begin{aligned}
&\mathcal{L}[\;(\;\mathbf{x}_k \quad \mathbf{x}_j\;)] = \sum_{i=1}^{n} \;_i\;(\;\mathbf{x}_k \quad \mathbf{x}_i\;) + \qquad k = 1 \qquad n \\
&\sum_{i=1}^{n} \;_i = 0
\end{aligned}
\tag{4}
$$

where is a constant related to .

2.2 RBF-HFD method

In the RBF-HFD method the accuracy of the approximation (1) is increased without increasing the size stencil. In this case, given a stencil with n nodes $\mathbf{x}_1 \; \mathbf{x}_2 \quad \mathbf{x}_n$ and a subset $\mathbf{x}_1 \; \mathbf{x}_2 \quad \mathbf{x}_{j\;1} \; \mathbf{x}_{j+1} \quad \mathbf{x}_m$ with $m < n$ nodes, the di erential operator $\mathcal{L}[\;]$ is approximated at $\mathbf{x} = \mathbf{x}_j$ by the formula

$$
\mathcal{L}[u(\mathbf{x}_j)] \quad \sum_{i=1}^{n} \;_i u(\mathbf{x}_i) + \sum_{p=1}^{m} \;_p \mathcal{L}[u(\mathbf{x}_p)] \tag{5}
$$

where $_i$ and $_p$ are the weighting coe cients. These coe cients are computed using Hermite RBF interpolants,

$$
u(\mathbf{x}) = \sum_{i=1}^{n} \;_i\;(\;\mathbf{x} \quad \mathbf{x}_i\;) + \sum_{p=1}^{m} \;_p \mathcal{L}[\;(\;\mathbf{x} \quad \mathbf{x}_p\;)] \tag{6}
$$

In this case, the unknown weighting coe cients can be determined by solving the system of linear equations (7) obtained after substituing (6) in (5) and operating,

$$
\begin{aligned}
&\mathcal{L}[\;(\;\mathbf{x}_k \quad \mathbf{x}_j\;)] = \sum_{i=1}^{n} \;_i\;(\;\mathbf{x}_k \quad \mathbf{x}_i\;) + \sum_{p=1}^{m} \;_p \mathcal{L}[\;(\;\mathbf{x}_k \quad \mathbf{x}_p\;)] \\
&\mathcal{L}\mathcal{L}[\;(\;\mathbf{x}_s \quad \mathbf{x}_j\;)] = \sum_{i=1}^{n} \;_i \mathcal{L}[\;(\;\mathbf{x}_s \quad \mathbf{x}_i\;)] + \sum_{p=1}^{m} \;_p \mathcal{L}\mathcal{L}[\;(\;\mathbf{x}_s \quad \mathbf{x}_p\;)]
\end{aligned}
\tag{7}
$$

where $k = 1 \quad n$ and $s = 1 \quad m$. As in the previous section, a constant term ( ) should be added in the Hermitte RBF interpolant (6) to guarantee that these RBF-HFD formulas are exact for constants. In this case, the system of equations to be solved are

$$\mathcal{L}[\phi(\|\mathbf{x}_k - \mathbf{x}_j\|)] = \sum_{i=1}^{n} \alpha_i \phi(\|\mathbf{x}_k - \mathbf{x}_i\|) + \sum_{p=1}^{m} \beta_p \mathcal{L}[\phi(\|\mathbf{x}_k - \mathbf{x}_p\|)] + \gamma$$

$$\mathcal{L}\mathcal{L}[\phi(\|\mathbf{x}_s - \mathbf{x}_j\|)] = \sum_{i=1}^{n} \alpha_i \mathcal{L}[\phi(\|\mathbf{x}_s - \mathbf{x}_i\|)] + \sum_{p=1}^{m} \beta_p \mathcal{L}\mathcal{L}[\phi(\|\mathbf{x}_s - \mathbf{x}_p\|)] \quad (8)$$

$$\sum_{i=1}^{n} \alpha_i = 0$$

where $k = 1, \ldots, n$, $s = 1, \ldots, m$ and γ is a constant related to ε.

3 Weights and Truncation Error

In this section, we derive analytical expressions for the weights of RBF-FD and RBF-HFD formulas using Gaussians as RBFs,

$$\phi(\|\mathbf{x} - \mathbf{x}_j\|) = \exp\left(-\varepsilon^2 \|\mathbf{x} - \mathbf{x}_j\|^2\right) \quad (9)$$

where ε is the shape parameter. We consider RBF-FD formulas for first and second order derivatives in 1D, and for the Laplacian in 2D, using equispaced nodes in all cases. Only first and second order derivatives formulas in 1D are derived for the RBF-HFD method. The weights are functions of the inter node distance h and the shape parameter ε. They are obtained using Mathematica. Contrary to what happened with multiquadrics [1], in which case the weights were written as Taylor series expansions in powers of h, for Gaussians it is often possible to write them as short analytical formulas. These coefficients are then used to derive analytical expressions for the leading term of the local truncation error in the limit $h \ll 1$, which is defined as

$$\tau_n(\mathbf{x}_0) = \sum_{i=1}^{n} \alpha_i u(\mathbf{x}_i) - \mathcal{L}[u(\mathbf{x}_0)]$$

for the RBF-FD method and

$$\tau_n(\mathbf{x}_0) = \sum_{i=1}^{n} \alpha_i u(\mathbf{x}_i) + \sum_{p=1}^{m} \beta_p \mathcal{L}[u(\mathbf{x}_p)] - \mathcal{L}[u(\mathbf{x}_0)]$$

for the RBF-HFD method. In the tables we use the notation $O\left(h^r P_k(\varepsilon^2)\right)$ to indicate that the terms that have been neglected are of order $h^r \sum_{i=0}^{k} a_i \varepsilon^{2i}$, where a_i are constants.

3.1 RBF-FD formulas

To check the validity of the formulas given in this subsection, we use

$$u(\mathbf{x}) = \sin\left(||\mathbf{x}||^2\right),$$

as test function, where $||\mathbf{x}||$ is the euclidean norm. Equations (3) and (4) are used to compute the coefficients needed to approximate the corresponding operator $\mathcal{L}[\cdot]$ at $x_0 = 0.4$ and $\mathbf{x}_0 = (0.4, 0.4)$ in 1D and 2D, respectively. For each formula we compute the absolute value of the error as a function of the shape parameter ϵ and the node distance h, and compare it with the leading term of the local truncation error that we derive in the limit $\epsilon h \ll 1$.

3.1.1 First derivative

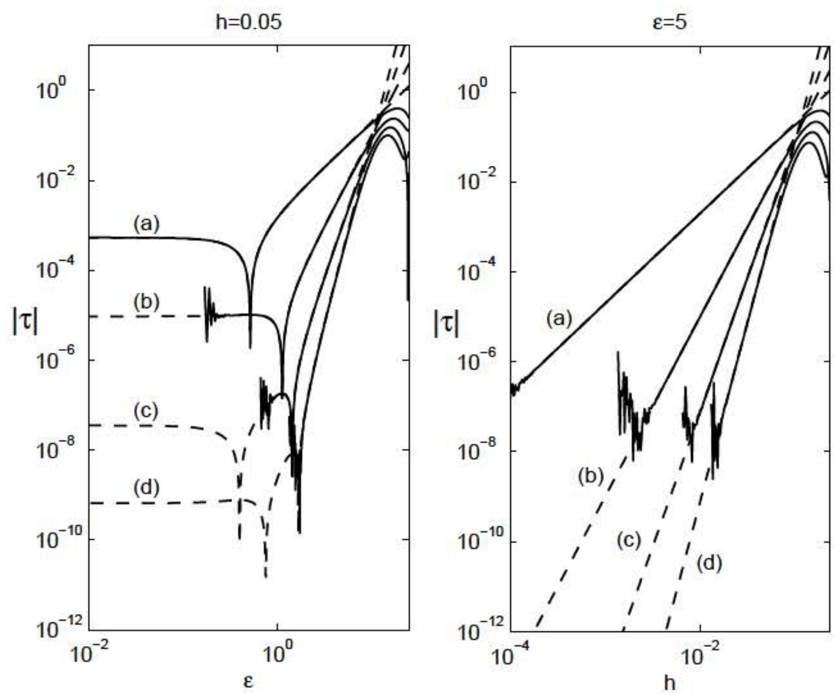

Figure 1: Local truncation error τ_n for the RBF-FD first derivative as function of ϵ (left side) and h (right side) using structured stencils with (a) $n = 3$, (b) $n = 5$, (c) $n = 7$, and (d) $n = 9$ nodes. Solid lines: local truncation error computed solving numerically (3). Dashed lines: leading order formulas of the errors given in Table 1.

Table 1: RBF-FD rst derivative.

Three nodes	
0	0
1	$\frac{1}{2}\ {}^2h\,(\mathrm{csch}\,(\ {}^2h^2)+\mathrm{sech}\,(\ {}^2h^2))$
3	$\frac{h^2}{6}\ \ u\ \ (x_0)+6\ {}^2u\ (x_0)\ \ +O\,(h^4P_2(\ {}^2))$
Five nodes	
0	0
1	${}^2h\ \ 1+e^{2\ {}^2h^2}\ \ \mathrm{csch}\,(3\ {}^2h^2)$
2	$\frac{{}^2he^{4\ {}^2h^2}}{\sinh(2\ {}^2h^2)+\sinh(4\ {}^2h^2)+\sinh(6\ {}^2h^2)}$
5	$\frac{h^4}{30}\ \ u^{(V)}(x_0)+20\ {}^2u\ \ (x_0)+60\ {}^4u\ (x_0)\ \ +O\,(h^6P_3(\ {}^2))$
Seven nodes	
0	0
1	${}^2h\ \ e^{3\ {}^2h^2}+2\cosh\,(\ {}^2h^2)\ \ \mathrm{csch}\,(4\ {}^2h^2)$
2	$\frac{{}^2he^{2\ {}^2h^2}\ \ 1+e^{2\ {}^2h^2}+e^{4\ {}^2h^2}}{\sinh(2\ {}^2h^2)+\sinh(4\ {}^2h^2)+\sinh(6\ {}^2h^2)+\sinh(8\ {}^2h^2)}$
+3	$\frac{{}^2he^{9\ {}^2h^2}}{\sinh(2\ {}^2h^2)+2\sinh(4\ {}^2h^2)+2\sinh(6\ {}^2h^2)+2\sinh(8\ {}^2h^2)+\sinh(10\ {}^2h^2)+\sinh(12\ {}^2h^2)}$
3	$\frac{{}^2he^{9\ {}^2h^2}\mathrm{csch}\left(6\ {}^2h^2\right)}{2(1+2\cosh(2\ {}^2h^2)+\cosh(4\ {}^2h^2)+\cosh(6\ {}^2h^2))}$
7	$\frac{h^6}{140}\ \ u^{(VII)}(x_0)+42\ {}^2u^{(V)}(x_0)+420\ {}^4u\ \ (x_0)+840\ {}^6u\ (x_0)\ \ +O\,(h^8P_4(\ {}^2))$
Nine nodes	
0	0
1	$\frac{4}{5h}\ \ \frac{4\ {}^2h}{5}\ \ \frac{14\ {}^4h^3}{15}\ \ \frac{6\ {}^6h^5}{5}\ \ \frac{191\ {}^8h^7}{90}+O\,(\ {}^{10}h^9)$
2	$\frac{1}{5h}\ \ \frac{4\ {}^2h}{5}\ \ \frac{4\ {}^4h^3}{15}\ \ \frac{16\ {}^6h^5}{5}\ \ \frac{104\ {}^8h^7}{45}+O\,(\ {}^{10}h^9)$
3	$\frac{4}{105h}\ \ \frac{12\ {}^2h}{35}\ \ \frac{34\ {}^4h^3}{35}\ \ \frac{18\ {}^6h^5}{35}\ \ \frac{531\ {}^8h^7}{70}+O\,(\ {}^{10}h^9)$
4	$\frac{1}{280h}\ \ \frac{2\ {}^2h}{35}\ \ \frac{38\ {}^4h^3}{105}\ \ \frac{32\ {}^6h^5}{35}\ \ \frac{316\ {}^8h^7}{315}+O\,(\ {}^{10}h^9)$
9	$\frac{h^8}{630}\ \ u^{(IX)}(x_0)+72\ {}^2u^{(VII)}(x_0)+1512\ {}^4u^{(V)}(x_0)+10080\ {}^6u\ \ (x_0)+15120\ {}^8u\ (x_0)\ \ +O\ \ h^{10}P_5(\ {}^2)$

Table 1 shows the weights and the corresponding local truncation errors for RBF-FD formulas to approximate the first derivative in 1D. Exact expressions are given for 3, 5 and 7 equispaced nodes. For 9 equispaced nodes the exact formulas are too long and therefore we only include their series expansions in the limit $\varepsilon h \ll 1$. The results for 3 and 5 nodes are in agreement with those previously derived in Appendix A of reference [4].

Figure 1 shows the corresponding error (solid line) for $n = 3, 5, 7$ and 9 when the weights are computed by solving numerically the linear system (3). This error is compared with the approximate error given by the formulas in Table 1 (dashed line). Notice that the agreement is excellent up to the point where the linear system to numerically compute the weights (3) becomes ill-conditioned and round-off errors deteriorate the accuracy of the numerical solution. However, it should be emphasized that, in the case of Gaussians, it is not necessary to numerically solve (3) in order to get the weights. Instead, the analytic formulas given in Table 1 can be directly used. In that case the actual local error is undistinguishable from the approximate error given by the formulas in Table 1. The left part of Figure 1 shows the absolute value of the error as a function of the shape parameter for $h = 0.05$. The accuracy increases with decreasing ε. For small ε (flat RBFs) it is well known that RBF-FD formulas approach standard finite difference formulas [7]. This fact can be clearly observed in the figure which shows how the error approaches the standard finite difference error when $\varepsilon \to 0$.

Notice also that there is a range of values of the shape parameter, ε, for which RBF-FD formulas are more accurate than standard finite differences. In particular, there is an optimal value, ε^+, for which the local truncation error is zero to leading order. Since the value of ε^+ can be accurately estimated from the formulas in Table 1, it is possible to use the RBF-FD method to accurately solve PDE problems following the same approach described in references [2, 3] for multiquadrics.

The right part of Figure 1 shows the absolute value of the error as a function of the inter node distance h for $\varepsilon = 5$. Notice that the error behaves as $O(h^{n-1})$ in agreement with the formulas in Table 1.

3.1.2 Second derivative

Table 2 shows the weights and the corresponding truncation errors for RBF-FD formulas to approximate the second derivative in 1D using the standard formulation which is not exact for constants (3). As in the previous case, exact expressions are given for 3, 5 and 7 equispaced nodes. For 9 equispaced nodes only their series expansions in the limit $\varepsilon h \ll 1$ are included.

Figure 2 shows the numerical error (solid line) in the approximation of

Table 2: RBF-FD second derivative: non exact for constants

	Three nodes
0	$2 \quad {}^2 + \; {}^4 h^2 \operatorname{csch}^2 (\; {}^2 h^2)$
1	${}^4 h^2 (1 + \coth (\; {}^2 h^2)) \operatorname{csch} (\; {}^2 h^2)$
3	$\frac{h^2}{12} \quad u^{(IV)}(x_0) + 12 \; {}^2 u \;\; (x_0) + 12 \; {}^4 u(x_0) \quad + O\left(h^4 P_3(\; {}^2)\right)$
	Five nodes
0	$\frac{1}{2} \quad {}^4 h^2 \quad \operatorname{sech}^2 (\; {}^2 h^2) \quad 5\operatorname{csch}^2 (\; {}^2 h^2) \quad 4 \; {}^2$
1	$\frac{4 \; {}^4 h^2 \cosh\left(\; {}^2 h^2\right) \coth\left(\; {}^2 h^2\right)\left(\coth\left(\; {}^2 h^2\right)+1\right)}{2\cosh(2 \; {}^2 h^2)+1}$
2	$\frac{{}^4 h^2 e^{4 \; {}^2 h^2} \operatorname{csch}^2\left(2 \; {}^2 h^2\right)}{2\cosh(2 \; {}^2 h^2)+1}$
5	$\frac{h^4}{90} \quad u^{(VI)}(x_0) + 30 \; {}^2 u^{(IV)}(x_0) + 180 \; {}^4 u \;\; (x_0) + 120 \; {}^6 u(x_0) \quad + O\left(h^6 P_4(\; {}^2)\right)$
	Seven nodes
0	$\frac{1}{18} \; {}^2 \quad \frac{32 \; {}^2 h^2\left(\cosh\left(2 \; {}^2 h^2\right)+2\right)}{(2\cosh(2 \; {}^2 h^2)+1)^2} \quad 49 \; {}^2 h^2 \operatorname{csch}^2 (\; {}^2 h^2) + 9 \; {}^2 h^2 \operatorname{sech}^2 (\; {}^2 h^2) \quad 36$
1	$\frac{1}{2} \; {}^4 h^2 (\coth (\; {}^2 h^2) + 1) \operatorname{csch} (\; {}^2 h^2) (\operatorname{sech} (2 \; {}^2 h^2) + 2)$
2	$\frac{{}^4 h^2 e^{2 \; {}^2 h^2} \quad e^{2 \; {}^2 h^2} + e^{4 \; {}^2 h^2} + 1 \quad \operatorname{csch}^2\left(2 \; {}^2 h^2\right)}{2\cosh(2 \; {}^2 h^2) + 2\cosh(4 \; {}^2 h^2) + 1}$
3	$\frac{{}^4 h^2 e^{9 \; {}^2 h^2} \operatorname{csch}^2\left(3 \; {}^2 h^2\right)}{2(2\cosh(2 \; {}^2 h^2) + \cosh(4 \; {}^2 h^2) + \cosh(6 \; {}^2 h^2) + 1)}$
7	$\frac{h^6}{560} \quad u^{(VIII)}(x_0) + 56 \; {}^2 u^{(VI)}(x_0) + 840 \; {}^4 u^{(IV)}(x_0) + 3360 \; {}^6 u \;\; (x_0) + 1680 \; {}^8 u(x_0) \quad + O \quad h^8 P_5(\; {}^2)$
	Nine nodes
0	$\frac{205}{72h^2} \quad 2 \; {}^2 + \frac{8h^2 \; {}^4}{3} \quad 4h^6 \; {}^8 + O\left(h^{10} \; {}^{12}\right)$
1	$\frac{8}{5h^2} + \frac{8 \; {}^2}{5} \quad \frac{4h^2 \; {}^4}{3} \quad \frac{28h^4 \; {}^6}{15} + \frac{269h^6 \; {}^8}{75} + \frac{191h^8 \; {}^{10}}{45} + O\left(h^{10} \; {}^{12}\right)$
2	$\frac{1}{5h^2} \quad \frac{4 \; {}^2}{5} \quad \frac{8h^2 \; {}^4}{15} + \frac{32h^4 \; {}^6}{15} + \frac{152h^6 \; {}^8}{75} \quad \frac{352h^8 \; {}^{10}}{45} + O\left(h^{10} \; {}^{12}\right)$
2	$\frac{8}{315h^2} + \frac{8 \; {}^2}{35} + \frac{76h^2 \; {}^4}{105 \; 9} + \frac{12h^4 \; {}^6}{35} \quad \frac{79h^6 \mathrm{ep}^8}{25} \quad \frac{153h^8 \; {}^{10}}{35} + O\left(h^{10} \; {}^{12}\right)$
4	$\frac{1}{560h^2} \quad \frac{{}^2}{35} \quad \frac{4h^2 \; {}^4}{21} \quad \frac{64h^4 \; {}^6}{105} \quad \frac{34h^6 \; {}^8}{75} + \frac{992h^8 \; {}^{10}}{315} + O\left(h^{10} \; {}^{12}\right)$
9	$\frac{h^8}{3150} \quad u^{(X)}(x_0) + 90 \; {}^2 u^{(VIII)}(x_0) + 2520 \; {}^4 u^{(VI)}(x_0) + 25200 \; {}^6 u^{(IV)}(x_0) + 75600 \; {}^8 u \;\; (x_0) + 30240 \; {}^{10} u(x_0) \quad + O \quad h^{10} P_6(\; {}^2)$

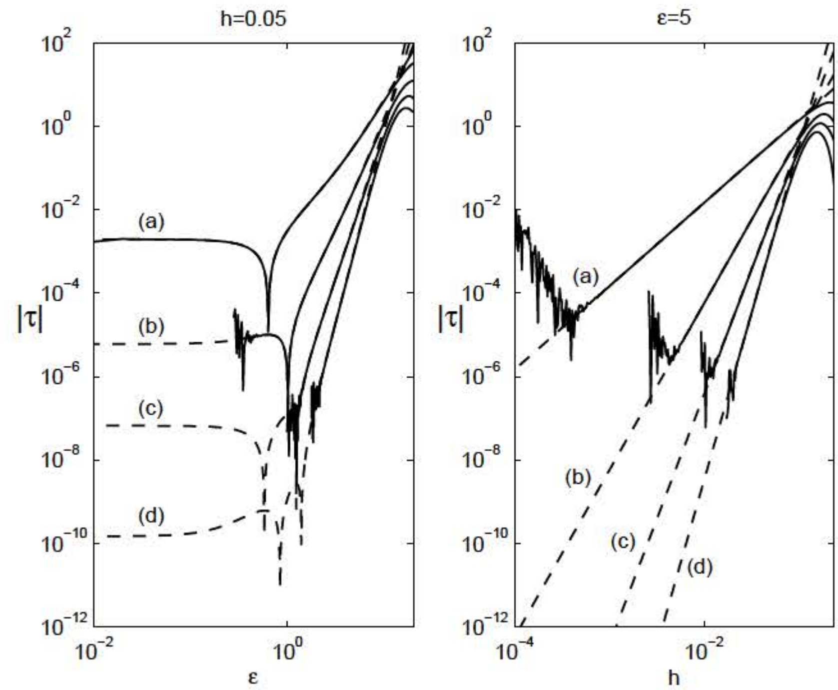

Figure 2: Same as Figure 1 but for the RBF-FD second derivative (non exact for constants).

the second derivative with $n = 3, 5, 7$ and 9 using the standard formulation (3) which is not exact for constants. The numerical results are compared with the approximate error given by the formulas in Table 2 (dashed line). The left part of Figure 2 shows the absolute value of the error as a function of the shape parameter for $h = 0.05$, and the right part shows the absolute value of the error as a function of the inter node distance h for $\epsilon = 5$. In the first case, the accuracy increases with decreasing ϵ and approaches standard finite differences for small ϵ. Notice that there is an optimal value, ϵ^+, for which the local truncation error is zero to leading order. In the second case, the error behaves as $O(h^{n-1})$ in agreement with the formulas in Table 2.

Table 3 shows the weights and the corresponding local truncation errors for RBF-FD formulas to approximate the second derivative in 1D using the standard formulation which is exact for constants (4). In this case, exact expressions are only given for 3 equispaced nodes. For 5,7 and 9 equispaced nodes we only include their series expansions in the limit $\epsilon h \ll 1$. Figure 3 shows the corresponding error (solid line) for $n = 3, 5, 7, 9$, and compares it with the approximate error given by the formulas in table 3 (dashed line). Both results coincide until the system of equations (3) be-

Table 3: RBF-FD second derivative: exact for constants

Three nodes	
0	$\frac{4\ {}^2 e^{3\ {}^2 h^2}\ \ 2\ {}^2 h^2 + e\ {}^{2} h^2\ \ 1}{4e^{3\ {}^2 h^2} + 3e^{4\ {}^2 h^2} + 1}$
1	$\frac{2\ {}^2 e^{3\ {}^2 h^2}\ \ 2\ {}^2 h^2 + e\ {}^{2} h^2\ \ 1}{4e^{3\ {}^2 h^2} + 3e^{4\ {}^2 h^2} + 1}$
3	$\frac{h^2}{12}\ \ u^{(IV)}(x_0) + 10\ {}^2 u\ \ (x_0)\ \ + O\left(h^4 P_2(\ {}^2)\right)$
Five nodes	
0	$\frac{5}{2h^2}\quad \frac{28\ {}^2}{15} + \frac{83h^2\ {}^4}{90} + O\left(h^4\ {}^6\right)$
1	$\frac{4}{3h^2} + \frac{56\ {}^2}{45}\quad \frac{13h^2\ {}^4}{135} + O\left(h^4\ {}^6\right)$
2	$\frac{1}{12h^2}\quad \frac{14\ {}^2}{45}\quad \frac{197h^2\ {}^4}{540} + O\left(h^4\ {}^6\right)$
5	$\frac{h^4}{90}\ \ u^{(VI)}(x_0) + 28\ {}^2 u^{(IV)}(x_0) + 140\ {}^4 u\ \ (x_0)\ \ + O\left(h^6 P_3(\ {}^2)\right)$
Seven nodes	
0	$\frac{49}{18h^2}\quad \frac{27\ {}^2}{14} + \frac{237h^2\ {}^4}{140} + \frac{199h^4\ {}^6}{300} + O\left(h^6\ {}^8\right)$
1	$\frac{3}{2h^2} + \frac{81\ {}^2}{56}\quad \frac{333h^2\ {}^4}{560}\quad \frac{533h^4\ {}^6}{400} + O\left(h^6\ {}^8\right)$
2	$\frac{3}{20h^2}\quad \frac{81\ {}^2}{140}\quad \frac{801h^2\ {}^4}{1400} + \frac{127h^4\ {}^6}{200} + O\left(h^6\ {}^8\right)$
3	$\frac{1}{90h^2} + \frac{27\ {}^2}{280} + \frac{897h^2\ {}^4}{2800} + \frac{439h^4\ {}^6}{1200} + O\left(h^6\ {}^8\right)$
7	$\frac{h^6}{560}\ \ u^{(VIII)}(x_0) + 54\ {}^2 u^{(VI)}(x_0) + 756\ {}^4 u^{(IV)}(x_0) + 2520\ {}^6 u\ \ (x_0)\ \ + O\left(h^8 P_4(\ {}^2)\right)$
Nine nodes	
0	$\frac{205}{72h^2}\quad \frac{88\ {}^2}{45} + \frac{254h^2\ {}^4}{105} + \frac{358h^4\ {}^6}{525}\quad \frac{173561h^6\ {}^8}{33075} + O\left(h^8\ {}^{10}\right)$
1	$\frac{8}{5h^2} + \frac{352\ {}^2}{225}\quad \frac{124h^2\ {}^4}{105}\quad \frac{1832h^4\ {}^6}{875} + \frac{569729h^6\ {}^8}{165375} + O\left(h^8\ {}^{10}\right)$
2	$\frac{1}{5h^2}\quad \frac{176\ {}^2}{225}\quad \frac{284h^2\ {}^4}{525} + \frac{1716h^4\ {}^6}{875} + \frac{375542h^6\ {}^8}{165375} + O\left(h^8\ {}^{10}\right)$
2	$\frac{8}{315h^2} + \frac{352\ {}^2}{1575} + \frac{52h^2\ {}^4}{75} + \frac{6344h^4\ {}^6}{18375}\quad \frac{457057h^6\ {}^8}{165375} + O\left(h^8\ {}^{10}\right)$
4	$\frac{1}{560h^2}\quad \frac{44\ {}^2}{1575}\quad \frac{19h^2\ {}^4}{105}\quad \frac{3391h^4\ {}^6}{6125}\quad \frac{108623h^6\ {}^8}{330750} + O\left(h^8\ {}^{10}\right)$
9	$\frac{h^8}{3150}\ \ u^{(X)}(x_0) + 88\ {}^2 u^{(VIII)}(x_0) + 2376\ {}^4 u^{(VI)}(x_0) + 22176\ {}^6 u^{(IV)}(x_0) + 55440\ {}^8 u\ \ (x_0)\ \ + O\ \ h^{10} P_5(\ {}^2)$

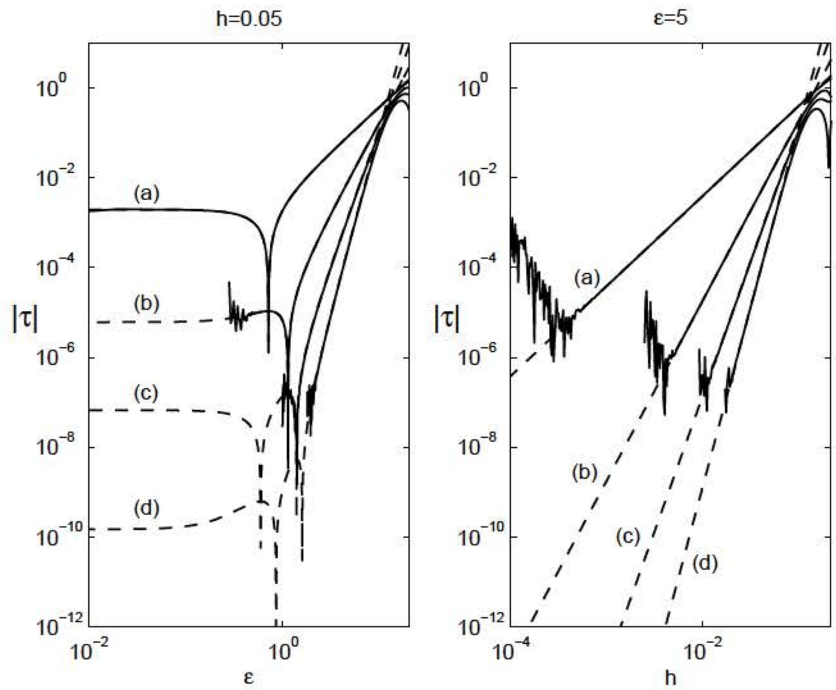

Figure 3: Same as Figure 1 but for the RBF-FD second derivative (exact for constants).

comes ill-conditioned. As in the previous cases, the existence of an optimal shape parameter, ϵ^+ which makes the error zero to leading order, can be clearly observed.

For $h \ll 1$ the error resulting from the formulation which is exact for constants (4) and from the formulation that is not exact (3) coincide (see figures 2 and 3 and tables 2 and 3). Notice however, that the error corresponding to the formulation which is non exact for constants (table 2) contains some extra terms. For instance, in the case of three nodes, the error for the non exact case includes a term proportional to ϵ^4 while the error corresponding to the exact case does not (table 3). Thus, for values of ϵ of order unity or larger, the two formulations may differ significantly.

3.1.3 Laplacian

Tables 4 and 5 show the weights and the corresponding local truncation error for the RBF-FD laplacian formulas with 5 and 9 nodes (non exact and exact for constants, respectively). Notice that in the non exact case (Table 4), the expressions for the weights and the local error are equivalent in both cases.

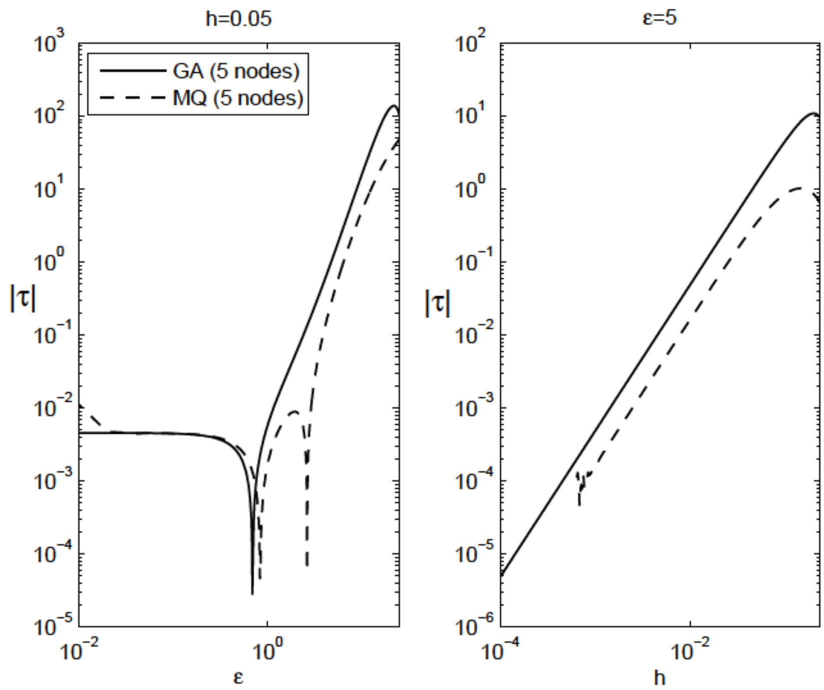

Figure 4: Local truncation error τ for the RBF-FD laplacian (non exact for constants) as function of ϵ (left side) and h (right side) using $n = 5$ structured stencils. Solid line: Gaussians. Dashed line: multiquadrics.

Figures 4 and 5 show the local truncation error obtained using the corresponding analytical weights of Tables 4 and 5 for $n = 5$ (solid line) and compare it with the local truncation errors obtained numerically with multiquadrics (dashed line). As it is shown in the figures, the rates of convergence are equivalent in both cases. This is due to the fact that the local truncation errors are polynomials of the same degree n in the shape parameter ϵ (see Tables 4 and 5 and [1]). As $\epsilon \to 0$, the local truncation error becomes equivalent since they both approach to standard finite differences.

Regarding accuracy, there are not advantages on using either multiquadrics or Gaussians, in general. However, for a specific function there might be significant differences associated to the fact that the location and/or the existence of the optimal shape parameter will change from using either one or the other. In this particular example, the error using multiquadrics is slightly smaller than with Gaussians. Note that the location of the optimal shape parameter is different.

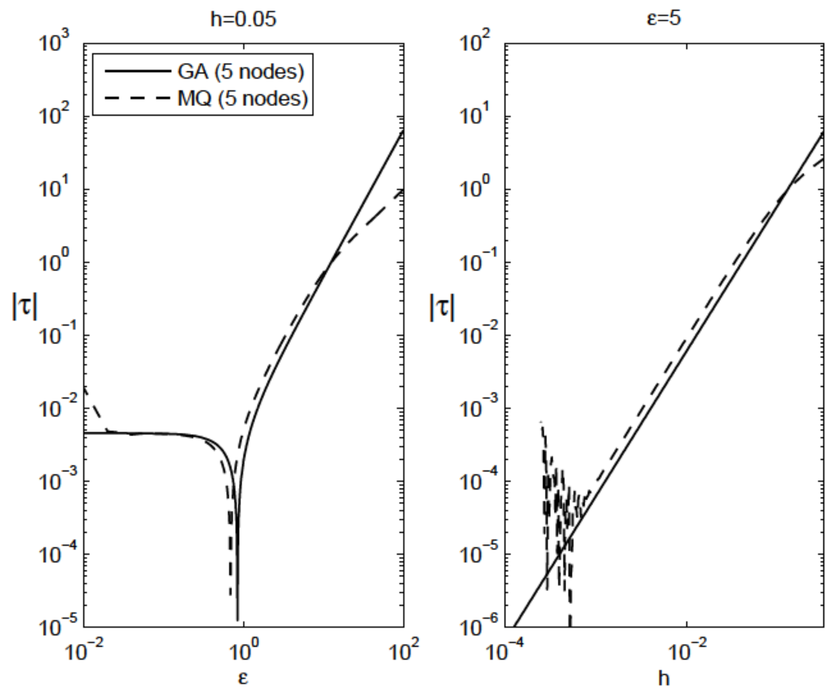

Figure 5: Same as Figure 4 but for the RBF-FD laplacian (exact for constants)

Table 4: RBF-FD laplacian: non exact for constants. Notice that ${}_9 = {}_5$.

Five nodes	
${}_0$	$4 \quad {}^2 + \ {}^4 h^2 \operatorname{csch}^2 (\ {}^2 h^2)$
${}_{1\ 2\ 3\ 4}$	${}^4 h^2 \left(1 + \coth (\ {}^2 h^2)\right) \operatorname{csch} (\ {}^2 h^2)$
${}_5$	$\frac{h^2}{12} \ u^{(4\,0)}(\mathbf{x}_0) + u^{(0\,4)}(\mathbf{x}_0) \ + \ {}^2 h^2 \ u^{(2\,0)}(\mathbf{x}_0) + u^{(0\,2)}(\mathbf{x}_0) \ + 2 \ {}^4 h^2 u(\mathbf{x}_0) + O\left(h^4 P_3(\ {}^2)\right)$
Nine nodes	
${}_0$	$4 \quad {}^2 + \ {}^4 h^2 \operatorname{csch}^2 (\ {}^2 h^2)$
${}_{1\ 2\ 3\ 4}$	${}^4 h^2 \left(1 + \coth (\ {}^2 h^2)\right) \operatorname{csch} (\ {}^2 h^2)$
${}_{5\ 6\ 7\ 8}$	0
${}_9$	$\frac{h^2}{12} \ u^{(4\,0)}(\mathbf{x}_0) + u^{(0\,4)}(\mathbf{x}_0) \ + \ {}^2 h^2 \ u^{(2\,0)}(\mathbf{x}_0) + u^{(0\,2)}(\mathbf{x}_0) \ + 2 \ {}^4 h^2 u(\mathbf{x}_0) + O\left(h^4 P_3(\ {}^2)\right)$

Table 5: RBF-FD laplacian: exact for constants

Five nodes	
0	$\frac{16\ {}^2e^{3\ {}^2h^2}\ \ {}^2h^2+e^{\ {}^2h^2}\ \ 1}{2e^{2\ {}^2h^2}\ \ 8e^{3\ {}^2h^2}+5e^{4\ {}^2h^2}+1}$
1 2 3 4	$\frac{4\ {}^2e^{3\ {}^2h^2}\ \ {}^2h^2+e^{\ {}^2h^2}\ \ 1}{2e^{2\ {}^2h^2}\ \ 8e^{3\ {}^2h^2}+5e^{4\ {}^2h^2}+1}$
5	$\frac{h^2}{12}\ \ u^{(4\,0)}(\mathbf{x}_0)+u^{(0\,4)}(\mathbf{x}_0)\ \ +\frac{3}{4}\ {}^2h^2\ \ u^{(2\,0)}(\mathbf{x}_0)+u^{(0\,2)}(\mathbf{x}_0)\ \ +\ O\left(h^4P_2(\ {}^2)\right)$
Nine nodes	
0	$\frac{16\ {}^2e^{3\ {}^2h^2}\ \ {}^2h^2+e^{\ {}^2h^2}\ 3\ {}^2h^2+e^{\ {}^2h^2}\ 2\ {}^2h^2+e^{\ {}^2h^2}\ \ 2\ {}^2h^2+e^{\ {}^2h^2}\ \ 7\ {}^2h^2\ \ e^{\ {}^2h^2}\ \ {}^2h^2+2e^{\ {}^2h^2}+1\ +4\ +3\ \ 1\ \ 2\ \ 1}{e^{\ {}^2h^2}\ \ 1^{\ 3}\ 3e^{\ {}^2h^2}+5e^{2\ {}^2h^2}+3e^{3\ {}^2h^2}+1^{\ 2}}$
1 2 3 4	$\frac{4\ {}^2e^{3\ {}^2h^2}\ \ \ {}^2h^2+e^{5\ {}^2h^2}+e^{\mathrm{ep}^2h^2}\left(1\ \ 2\ {}^2h^2\right)+2e^{3\ {}^2h^2}\left(\ {}^2h^2\ \ 1\right)+e^{4\ {}^2h^2}\left(5\ {}^2h^2\ \ 1\right)+1}{\left(e^{\ {}^2h^2}\ \ 1\right)^3\left(e^{\ {}^2h^2}+1\right)\left(2e^{\ {}^2h^2}+3e^{2\ {}^2h^2}+1\right)^2}$
5 6 7 8	$\frac{4\ {}^2e^{6\ {}^2h^2}\ \ e^{2\ {}^2h^2}\left(\ \ 4\ {}^2h^2+2\sinh\left(\ {}^2h^2\right)+1\right)\ \ 1}{\left(e^{\ {}^2h^2}\ \ 1\right)^3\left(3e^{\ {}^2h^2}+5e^{2\ {}^2h^2}+3e^{3\ {}^2h^2}+1\right)^2}$
9	$\frac{h^2}{36}\ \ 3u^{(4\,0)}(\mathbf{x}_0)\ \ \ 2u^{(2\,2)}(\mathbf{x}_0)+3u^{(0\,4)}(\mathbf{x}_0)\ \ +\frac{2}{3}\ {}^2h^2\ \ u^{(0\,2)}(\mathbf{x}_0)+u^{(2\,0)}(\mathbf{x}_0)\ \ +\ O\left(h^4P_2(\ {}^2)\right)$

Table 6: RBF-HFD rst derivative

Three nodes	
0	0
1	$\dfrac{2\ {}^2he^{3\ {}^2h^2}\quad 4\ {}^2h^2+e^{4\ {}^2h^2}\quad 1}{8\ {}^2h^2e^{4\ {}^2h^2}+e^{8\ {}^2h^2}\quad 1}$
1	$\dfrac{e^{\ {}^2h^2}\left(2\ {}^2h^2\cosh\left(2\ {}^2h^2\right)\quad \sinh\left(2\ {}^2h^2\right)\right)}{4\ {}^2h^2\quad \sinh(4\ {}^2h^2)}$
3	$\frac{1}{120}h^4u^{(V)}(x_0)\quad \frac{1}{6}\ {}^2h^4u^{(III)}(x_0)\quad \frac{1}{2}\ {}^4h^4u\ (x_0)+O\left(h^6P_3(\ {}^2)\right)$

3.2 RBF-HFD formulas

To check the validity of the formulas given in this subsection, we use again

$$u(x) = \sin\ x^2$$

as test function, and use equations (7) and (8) to numerically compute the coe cients needed to approximate the rst and second derivatives at $x_0 = 1$ using the 1D stencil of Figure (6), where the double circle represents the subset for these equations.

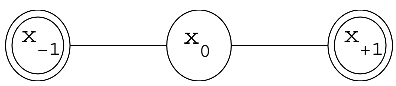

Figure 6: RBF-HFD stencil

For each formula we compute the absolute value of the error as a function of the shape parameter and the node distance h, and compare it with the leading term of the local truncation error in the limit h 1.

3.2.1 First derivative

Table 6 shows the exact values of the weights and the corresponding local truncation errors for RBF-HFD formulas to approximate the rst derivative in 1D using the three node stencil shown in gure 6.

Figure 7 shows the corresponding numerical error (solid line) and compares it with the approximate error given by the formula in Table 6 (dashed line). Notice that the agreement is excellent up to the point where the linear

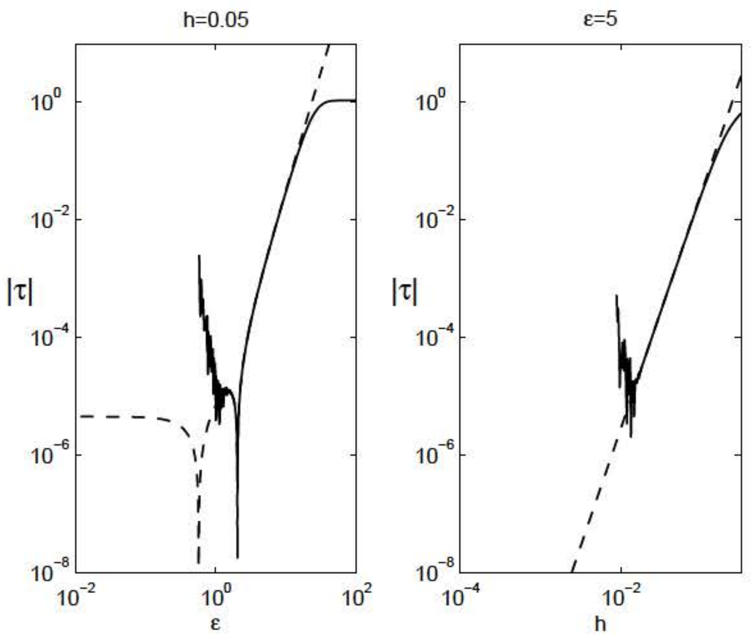

Figure 7: Local truncation error τ for the RBF-HFD first derivative as function of ϵ (left side) and h (right side) using the stencils of Figure 6. Solid line: local truncation error computed solving numerically (7). Dashed line: leading order formula of the error given in Table 6.

system to numerically compute the weights (7) becomes ill-conditioned and round-off errors deteriorate the accuracy of the numerical solution. The left part of Figure 7 shows the absolute value of the error as a function of the shape parameter for $h = 0.05$. The accuracy increases with decreasing ϵ.

It has been shown that RBF-FD formulas approach standard finite difference formulas in the limit $\epsilon \to 0$ [7]. Wright and Fornberg [21] studied RBF-HFD formulas and concluded that although there are not similar rigorous results for RBF-HFD formulas in the limit $\epsilon \to 0$, they expected similar results to hold. In fact, taking the limit $\epsilon \to 0$ in the weights given in table 6 results in $\alpha_{\pm 1} = \pm 3/4$, $\widetilde{\alpha}_{\pm 1} = -1/4$, which agrees with the results in Table 3, page 538 of [6].

It can be clearly observed that there are two distinct values of ϵ for which the error is zero to leading order. One of them occurs before the appearance of ill-conditioning and is accurately predicted by the approximate error formula. The other occurs in the region of ill-conditioning and, therefore, can not be seen with the numerical results.

The right part of Figure 7 shows the absolute value of the error as a function of the inter node distance h for $\epsilon = 5$. Notice that the error behaves as $O(h^4)$ in agreement with the formula in Table 6. Notice that the RBF-HFD formula with three nodes contains five weights (three of them independent). Thus, it should be compared to the RBF-FD formula for five nodes, which also contains five weights (three of them independent). Both have the same error dependence with h and with ϵ, although the RBF-HFD three nodes formula appears to be slightly more accurate than the RBF-FD five nodes formula. In fact, as $\epsilon \to 0$ the RBF-HFD local truncation error approaches $-(1/120)h^4u^{(5)}$ while the corresponding RBF-FD formula approaches $-(1/30)h^4u^{(5)}$.

3.2.2 Second derivative

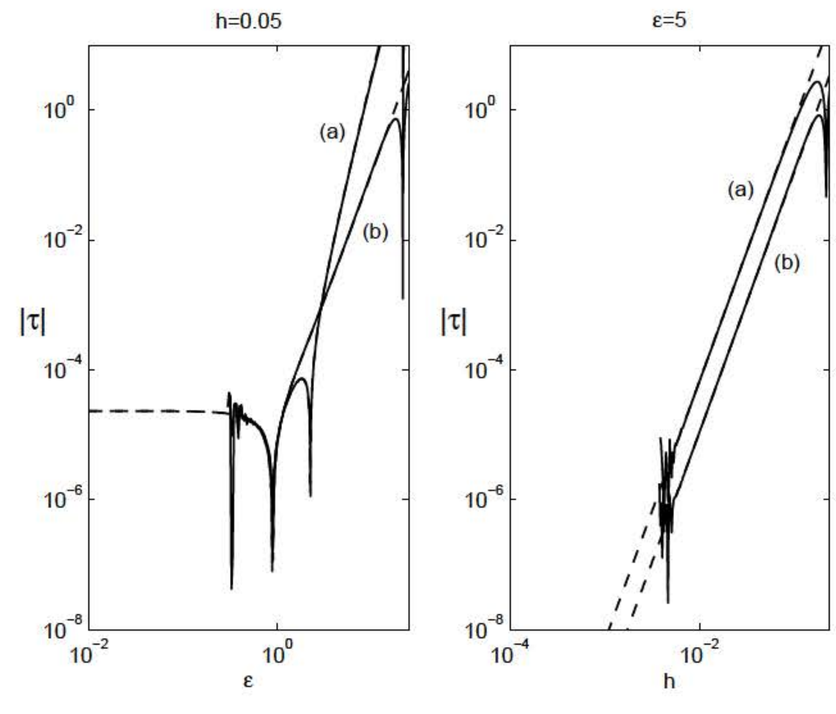

Figure 8: Same as Figure 7 but for the RBF-HFD second derivative: (a) formulation (7) non exact for constants, and (b) formulation (8) exact for constants.

Table 7 shows the weights and the corresponding local truncation errors to approximate the second derivative in 1D using the three node stencil shown in figure 6. Results are shown both for the formulation which is not exact for constants (7) and for the formulation which is exact for constants (8). In this

Table 7: RBF-HFD second derivative

	Three nodes: non exact for constants
0	$\frac{2\ {}^2\quad 16\ {}^2h^2+e^{8\ {}^2h^2}+2e^{4\ {}^2h^2}\ 1\ \ 4\ {}^2h^2\ {}^2+e^{6\ {}^2h^2}\ 8\ {}^6h^6\ \ 20\ {}^4h^4+8\ {}^2h^2\ \ 2\ +e^{2\ {}^2h^2}\ 72\ {}^6h^6\ \ 52\ {}^4h^4+24\ {}^2h^2\ \ 2\ +1}{16\ {}^2h^2+e^{8\ {}^2h^2}+2e^{4\ {}^2h^2}\ 1\ \ 4\ {}^2h^2\ {}^2+e^{2\ {}^2h^2}\ \ 36\ {}^4h^4+32\ {}^2h^2\ \ 2\ \ 2e^{6\ {}^2h^2}\ 2\ {}^4h^4+1\ +1}$
1	$\frac{2\ {}^2e^{3\ {}^2h^2}\ \ 48\ {}^6h^6\ \ 6\ {}^4h^4\ \ 10\ {}^2h^2+e^{4\ {}^2h^2}\left(2\ {}^4h^4\ \ 2\ {}^2h^2+1\right)\ \ 2e^{2\ {}^2h^2}\left(8\ {}^4h^4\ \ 6\ {}^2h^2+1\right)+1}{16\ {}^2h^2+e^{8\ {}^2h^2}+2e^{4\ {}^2h^2}(1\ \ 4\ {}^2h^2)^2+e^{2\ {}^2h^2}(\ \ 36\ {}^4h^4+32\ {}^2h^2\ \ 2)\ \ 2e^{6\ {}^2h^2}(2\ {}^4h^4+1)+1}$
1	$\frac{e^{3\ {}^2h^2}\ \ 6\ {}^4h^4\ \ 4\ {}^2h^2+e^{2\ {}^2h^2}\left(8\ {}^2h^2\ \ 2\right)+e^{4\ {}^2h^2}\left(2\ {}^4h^4\ \ 4\ {}^2h^2+1\right)+1}{16\ {}^2h^2+e^{8\ {}^2h^2}+2e^{4\ {}^2h^2}(1\ \ 4\ {}^2h^2)^2+e^{2\ {}^2h^2}(\ \ 36\ {}^4h^4+32\ {}^2h^2\ \ 2)\ \ 2e^{6\ {}^2h^2}(2\ {}^4h^4+1)+1}$
3	$\frac{1}{200}h^4u^{(VI)}(x_0)\quad \frac{3}{20}\ {}^2h^4u^{(IV)}(x_0)\quad \frac{9}{10}\ {}^4h^4u\ \ (x_0)\quad \frac{3}{5}\ {}^6h^4u(x_0)+O\left(h^6P_4(\ {}^2)\right)$
	Three nodes: exact for constants
0	$\frac{12}{5h^2}\quad \frac{84\ {}^2}{125}+\frac{3021h^2\ {}^4}{3125}+O\left(h^4\ {}^6\right)$
1	$\frac{6}{5h^2}+\frac{42\ {}^2}{125}\quad \frac{3021h^2\ {}^4}{6250}+O\left(h^4\ {}^6\right)$
1	$\frac{1}{10}\quad \frac{21h^2\ {}^2}{125}\quad \frac{677h^4\ {}^4}{6250}+O\left(h^4\ {}^6\right)$
3	$\frac{1}{200}h^4u^{(VI)}(x_0)\quad \frac{7}{50}\ {}^2h^4u^{(IV)}(x_0)\quad \frac{7}{10}\ {}^4h^4u\ \ (x_0)+O\left(h^6P_3(\ {}^2)\right)$

last case, only the series expansions of the coefficients in the limit h 1 are included. It should be pointed out, that in the limit 0 the weights given in table 7; $_0 =$ 12 $(5\,h^2)$, $_1 = 6$ $(5\,h^2)$, $_1 =$ 1 10, coincide with the results obtained with standard finite difference formulas (see Table 3, page 538 of [6]).

Figure 8 shows the numerical error (solid line) in the approximation of the second derivative with three equispaced nodes, using both the formulation which is non exact for constants (7) and the formulation which is exact for constants (8). The numerical results are compared with the approximate error given by the formulas in Table 7 (dashed line). There is an excellent agreement between the two results.

The left part of Figure 8 shows the absolute value of the error as a function of the shape parameter for $h = 0\ 05$, and the right part shows the absolute value of the error as a function of the inter node distance h for $= 5$. Notice, that in the case of the formulation which is not exact for constants, there are two values of for which the error is zero to leading order; $^+$ 2 2674 and $^+$ 0 8922. For the formulation which is exact for constants there is only one value, $^+$ 0 9129, for which the error is zero to leading order. Similarly to what happened with the first derivative, the error dependence on h and of these RBF-HFD formulas using three nodes (three independent weights), equals the corresponding error dependence of RBF-FD formulas using five nodes (three independent weights). However, in the limit 0 the accuracy of the RBF-HFD ($(1\ 200)h^4u^{(6)}$)appears to be slightly better than RBF-FD ($(1\ 90)h^4u^{(6)}$).

4 Conclusions

In this work we derive analytical expressions for the weights of RBF-FD and RBF-HFD formulas for first and second derivatives in 1D, and for the Laplacian in 2D using Gaussians as RBFs. Results are presented for 3, 5, 7 and 9 nodes in the case of RBF-FD formulas in 1D, and for 5 and 9 nodes in the case of RBF-FD formulas in 2D. For the case of RBF-HFD formulas we compute the weights for first and second order derivatives, using three equispaced nodes only. These weights are then used to derive analytical expressions for the leading order approximations to the local error in powers of the inter-node distance h. We show that the agreement of these formulas with the actual numerical error is very good.

We also show that for each differential operator, there is a range of values of the shape parameter for which RBF-FD formulas and RBF-HFD formulas are significantly more accurate than the corresponding conventional finite di erence formulas. In fact, very often there is an optimal value of the shape parameter $^{+}$ for which the error is zero to leading order. This value can be easily computed from the analytical expressions for the leading order approximations to the local error. Contrary to what is generally believed, this value is, to leading order, independent of the internodal distance and only dependent on the value of the function and its derivatives at the node.

The results presented in this paper can be used to e ciently solve PDE problems using RBF-FD or RBF-HFD formulas, by selecting a constant optimal value of the shape parameter (as was done in [2] for multiquadrics) or by selecting a node-dependent optimal shape parameter (as was done in [3] for multiquadrics).

It should be also emphasized that, contrary to what happened with multiquadrics [1], for Gaussians it is often possible to write the weights as exact analytical formulas. Thus, it is not necessary to numerically solve the linear system de ning the weights and, thereby, the problem of ill-conditioning which appears often when using these techniques, can be completely avoided.

5 Acknowledgements

This work has been supported by Spanish MICINN grants FIS2010-18473, CSD2010-00011 and by Madrid Autonomous Region grant S2009-1597. M.K. acknowledges Fundacion Caja Madrid for its nancial support.

References

[1] V. Bayona, M. Moscoso, M. Carretero, M. Kindelan, RBF-FD formulas and convergence properties, J. Comput. Phys. 229, (2010) 8281-8295.

[2] V. Bayona, M. Moscoso, M. Kindelan, Optimal constant shape parameter for multiquadric based RBF-FD method, J. Comput. Phys. 230, (2011) 7384-7399.

[3] V. Bayona, M. Moscoso, M. Kindelan, Optimal variable shape parameter for multiquadric based RBF-FD method, J. Comput. Phys. 231, (2012) 2466-2481.

[4] J. P. Boyd, L. Wang, Truncated Gaussian RBF Di erences are Always Inferior to Finite Di erences of the Same Stencil Width, Commun. Comput. Phys., 5 (2009),42-60.

[5] A. H.-D Cheng, Multiquadric and its shape parameter-A numerical investigation of error estimate, condition number, and round-off error by arbitrary precision computation, Engineering Analysis with Boundary Elements, 36 (2012) 220-239.

[6] L. Collatz, The numerical treatment of differential equations, Springer, Berlin (1960).

[7] T. A. Driscoll, B. Fornberg, Interpolation in the limit of increasingly flat radial basis functions, Comput. Math. Appl. 43 (2002) 413-422.

[8] G. E. Fasshauer, Meshfree Approximation Methods with MATLAB, World Scientific Publishing Co., Singapore (2007).

[9] O. Davydov and D. T. Oanh, Adaptive meshless centers and RBF stencils for Poisson equation, J. Comput. Phys. 230 (2011) 287-304.

[10] O. Davydov and D. T. Oanh, On Optimal Shape Parameter for Gaussian RBF-FD Approximation of Poisson Equation, University of Strathclyde Report (2011).

[11] N. Flyer, G. B. Wright, Transport Schemes on a Sphere Using Radial Basis Functions, J. Comput. Phys. 226 (2007) 1059-1084.

[12] B. Fornberg, E. Letho, Stabilization of RBF-generated finite difference methods for convective PDEs, J. Comput. Phys. 230 (2011) 2270-2285.

[13] E. J. Kansa, Multiquadrics, a scattered data approximation scheme with applications to computational fluid dynamics. I. Surface approximations and partial derivatives estimates, Comput. Math. Appl. 19 (1990) 127-145.

[14] E. J. Kansa, Multiquadrics, a scattered data approximation scheme with applications to computational fluid dynamics. II. Solutions to parabolic, hyperbolic and elliptic partial differential equations, Comput. Math. Appl. 19 (1990) 147-161.

[15] W. R. Madych, Miscellaneous error bounds for multiquadric and related interpolators, Comput. Math. Appl. 24 (1992) 121-138.

[16] B. Seibold, Minimal positive stencils in meshfree finite difference methods, Comput. Methods Appl. Mech. Engrg. 198 (2008) 592-601.

[17] C. Shu, H. Ding, K.S. Yeo, Local radial basis function-based di erential quadrature method and its application to solve two-dimensional incompressible Navier-Stokes equations, Computer Methods in Applied Mechanics and Engineering 192 (2003) 941-954.

[18] A. I. Tolstykh and D. A. Shirobokov, On using radial basis functions in a nite di erence mode with applications to elasticity problems, Computational Mechanics 33, (2003) 68-79.

[19] H. Wendland, Scattered data approximation, Cambridge University Press (2005).

[20] G. B. Wright, Radial basis function interpolation: numerical and analytical developments, Ph.D. thesis, University of Colorado, Boulder (2003).

[21] G. B. Wright, B. Fornberg, Scattered node compact nite di erence-type formulas generated from radial basis functions, J. Comput. Phys. 212, (2006) 99-123.